

InP-based Photodetector Monolithically Integrated with 90° Hybrid for 100 Gbit/s Compact Coherent Receivers

Naoko INOUE*, Hideki YAGI, Ryuji MASUYAMA, Tomokazu KATSUYAMA, Yoshihiro YONEDA and Hajime SHOJI

Digital coherent transmission is a promising technology for the next generation 100 Gbit/s transmission systems, and the development of compact coherent receivers and other optical components is essential to realize smaller coherent transceivers. Using InP-based monolithic integration of a 90° hybrid and waveguide photodiodes (PDs), we have developed a photodetector that provides high responsivity and high reliability. The compact coherent receiver, employing these InP-based integration devices, achieved a high sensitivity and demodulation of 128 Gbit/s DP-QPSK modulated signals. These results reveal that the InP-based photodetector monolithically integrated with the 90° hybrid will contribute to the realization of compact coherent receivers for 100 Gbit/s and beyond transmission systems.

Keywords: coherent receiver, 90° hybrid, photodetector, butt-joint, selective regrowth

1. Introduction

The enhancement and diversification of internet applications are progressing with the wide use of smartphones and tablet PCs, the evolution of video streaming, and the growth of cloud services. Concurrently, the realization of high-speed and large-capacity optical transmission systems is expected under the increasing trends of data communication traffic. Digital coherent transmission is a promising technology for the next generation 100 Gbit/s transmission systems⁽¹⁾. The transmission system, which is quite different from the previous system, gives high-sensitivity by coherent detection. The use of a digital signal processor provides stable phase synchronization between signal light and local oscillator light, in addition to both adaptive polarization dispersion compensation and chromatic dispersion compensation. In recent years, application spaces of the coherent systems are spreading from long-haul networks to metro networks. Downsizing of transmission equipment is strongly required for next generation coherent systems. Optical Internetworking Forum (OIF)⁽¹⁾ defines the standard specifications for coherent transmission equipment⁽²⁾. Therefore, the development of compact coherent receivers and other optical components is essential to realize smaller coherent transceivers like CFP or CFP2⁽²⁾ (Fig. 1). In this review, we elaborate on the high-responsivity photodetector monolithically integrated with a 90° hybrid⁽³⁾ using InP-based monolithic integration key

technologies, and introduce the compact coherent receiver, employing these InP-based integration devices.

2. Downsizing of Coherent Receiver

A configuration of a coherent receiver is shown in Fig. 2. The optical signal processing part, which identifies four signals, is composed of a polarization beam splitter (PBS) and two 90° hybrids. The optical/electrical conversion part in subsequent stage, which detects each signal, is composed of four photodiodes (PDs) and transimpedance amplifier (TIA) pairs. These configurations, which are integrated onto a single package, are widely used for dual polarization-quadrature phase shift keying (DP-QPSK)⁽⁴⁾ and other modulation formats. The size of the 90° hybrid is the most important point for the downsizing of a coherent receiver. The benchmark for 90° hybrid technology is shown in Table 1. A silica-based planar lightwave circuit (PLC), which is a mature technology, is widely used⁽³⁾. The silica-based 90° hybrid is large, and the monolithic integration with PDs is also difficult. Therefore, the size of the 90° hybrid is the main limiting factor for the downsizing of a coherent receiver. Silicon (Si) photonics, which have received attention in recent years, give smaller size design,

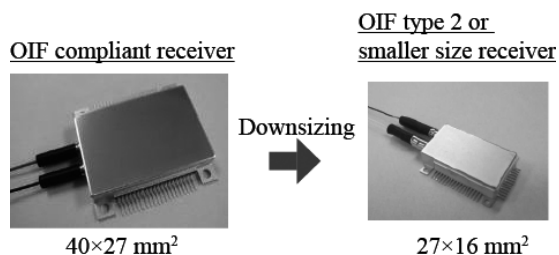


Fig. 1. Size of coherent receiver

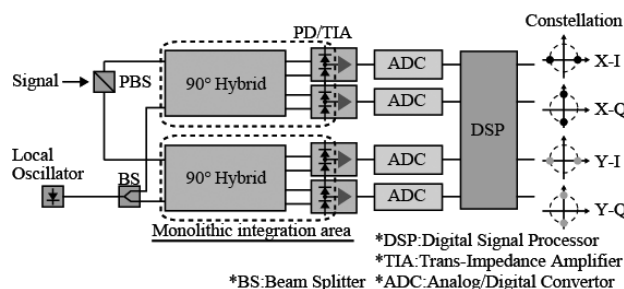
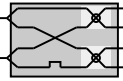
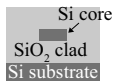


Fig. 2. Configuration of coherent receiver

Table 1. Benchmark for 90° hybrid technology

	Silica-PLC	InP-MMI	Si-Photonics
Waveguide structure	3 dB coupler 	4×4 MMI 	Si waveguide 
Size	× Large	○ Small	Smallest
Optical loss	○ Low	Fair	Fair
Monolithic integration with PDs	× No	Yes	Under study (Ge-PD)
Productivity	Good	Good	Under study

but the manufacturing technologies are still in the study phase, including a monolithic integration with PDs⁽⁴⁾. There are many things we should consider for commercial use. On the other hand, using the same material system as the existing optical devices, the InP-based MMI⁵, composed of semiconductor material system, can use the manufacturing technology of optical devices. An InP-based waveguide, which has larger refractive index difference between the core layer and the clad layer than a silica-based, is attractive to fabricating a compact 90° hybrid with a smaller bending radius. In addition, it allows the monolithic integration with PDs in subsequent stage, because both material systems match. The monolithic integration of 90° hybrid and PDs provides a significant reduction of excess loss in the optical coupling with a 90° hybrid. Therefore, it is effective for high-sensitivity in addition to the downsizing of a receiver module. From these viewpoints, the InP-based 90° hybrid is considered to be a promising candidate for the downsizing of a coherent receiver.

In this mission, we developed an InP-based photodetector in which are integrated four PDs at the end of the output waveguides, and realized the compact coherent receiver employing these InP-based integration devices.

3. Key Technologies for InP-based Monolithic Integration

InP-based monolithic integration technologies are essential to realize the photodetector integrated with a 90° hybrid. In this chapter, we elaborate on the key technologies on epitaxial growth and wafer process for optical integrated devices. These key technologies are shown in Fig. 3.

- (1) Dry etching technology, which is used to form deep-ridge waveguide⁶, provides precisely controlled mesa width, and smooth bending and branching. This technology enables a low transmission loss in waveguide, faithfully reproducing MMI design size and shape.
- (2) Butt-joint (BJ) epitaxial growth technology, in which the partial area patterned by insulating film is removed and the core layer of the different composition material is regrown, provides monolithic butt-coupling between heterogeneous cores for precise control of in-plane band-gap. This technology allows monolithic butt-coupling between the core layer of the 90° hybrid MMI and the optical absorption layer of PD.

- (3) Selective area regrowth technology provides selective regrowth to a specific portion of an integration device. This technology gives monolithic interconnection between a deep-ridge waveguide and a PD buried waveguide, and transition is realized with minimum optical loss/reflection.
- (4) Buried heterostructure (BH) regrowth technology for complicated structures provides flat regrowth over bending waveguides and couplers with various angles and facets. This technology gives surface without irregularities, and leads to easier electrode formation.

All these key technologies are realized on the 3-inch InP wafer. We fabricated the InP-based photodetector integrated with a 90° hybrid using these technologies.

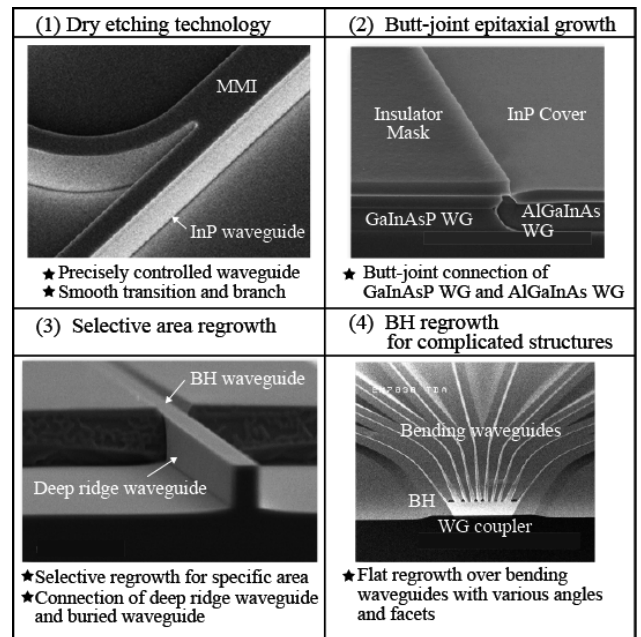


Fig. 3. Key technologies for monolithic integration

4. Device Structure and Fabrication Process

Figure 4 shows (a) the photomicrograph and (b) the schematic diagram for a completed InP-based photodetector integrated with the 90° hybrid⁽⁵⁾. The chip size was 4.1 mm × 1.6 mm. Significantly smaller size than 1/10 was achieved as compared to the silica-based 90° hybrid. The InP-based integrated chip consists of two parts, a GaInAsP core waveguide part, which functions as a 90° hybrid, and an InP/GaInAs waveguide PD part, which is arranged on four output ports of the 90° hybrid. The 90° hybrid part employs a deep-ridge waveguide structure suitable for obtaining a very small bending radius for fabricating compact integrated devices. It was comprised of the 2 × 4 MMI structure working as an 180° hybrid for in-phase relation and 2 × 2 MMI working for quadrature phase relation. Hence, the output channels from the 90° hybrid can be directly con-

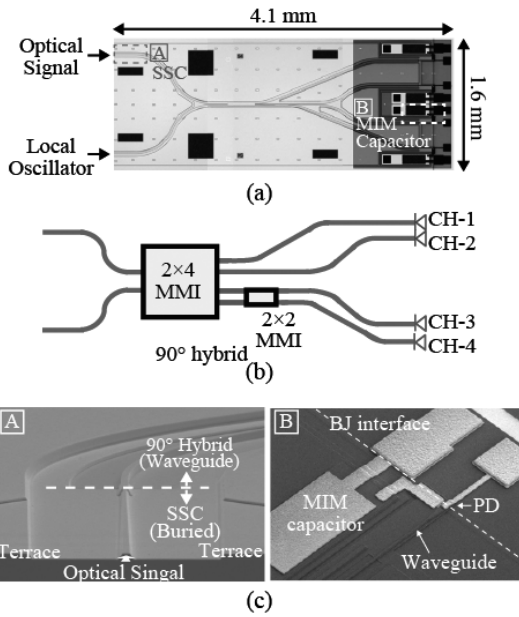


Fig. 4. InP-based photodetector integrated with the 90° hybrid (a) Photomicrograph, (b) schematic diagram for the InP-based photodetector monolithically integrated with the 90° hybrid consisting of MMI and (c) SEM image of [A] SSC section and [B] MIM capacitor section in (a)

ected to photodiodes without waveguide intersections, which induce excess loss, because the In-phase channels (CH-1 and CH-2) and the Quadrature channels (CH-3 and CH-4) are not spatially separated in this 90° hybrid structure. On the other hand, the InP/GaInAs waveguide PD part incorporates a buried waveguide structure which reduces dark current due to surface recombination current. This structure is formed by using a selective regrowth which was described in Section 3. At the same time, the spot-size converters (SSCs)⁷ are integrated by a buried waveguide structure on a short straight waveguide at the two optical input ports of the 90° hybrid in order to obtain higher optical coupling efficiency with the receiver module optics⁽⁶⁾.

In optical receiver modules, capacitors are usually assembled with PDs and TIAs to get good and stable characteristics. If it is possible to integrate the passive components in the optical modules on an identical substrate, the size and assembly cost of optical modules can be significantly reduced. Thus, metal-insulator-metal (MIM) capacitors were also monolithically integrated with the photodetector. MIM capacitors were formed on the GaInAsP core waveguide in which the flat surface with the epitaxially grown layer leads to uniform performance. The measured capacitance had good uniformity, and it was less than $\pm 2\%$. The dielectric breakdown voltage of the capacitor was larger than 100 V⁽⁷⁾.

Figure 5 shows the fabrication process of this integrated device. A pin-photodiode structure with a GaInAs absorption layer was prepared on a semi-insulating 3-inch InP wafer by organometallic vapor-phase-epitaxial (OMVPE) growth [Fig. 5 (a)]. The waveguide section with the GaInAsP core layer and the photodiode section were combined using the BJ regrowth process [Fig. 5 (b)]. Deep-ridge

waveguide stripes for the 90° hybrid and the photodiode array were simultaneously formed by standard optical i-line stepper lithography and reactive ion etching (RIE) techniques [Fig. 5 (c)]. The high uniformity of the deep-ridge waveguides was also confirmed from the scanning electron microscope (SEM), and the waveguide width variation over the 3-inch InP wafer has been reduced to less than $\pm 0.05 \mu\text{m}$ to attain the excess loss in MMI of less than 1.0 dB over the C-band. BH layers were selectively formed in photodiode sections to reduce the dark current and in SSC sections using OMVPE regrowth techniques [Fig. 5 (d)]. Then, electrodes were formed for the p- and n-side ohmic contacts. An air-bridge structure for the p-side electrode was also introduced to reduce parasitic capacitance in the photodiode section. Finally, an anti-reflection (AR) coating was applied on the optical input facet. The photomicrograph of the completed wafer, which were fabricated the InP-based photodetectors integrated with the 90° hybrid on a semi-insulating 3-inch InP wafer, is shown in **Photo. 1**.

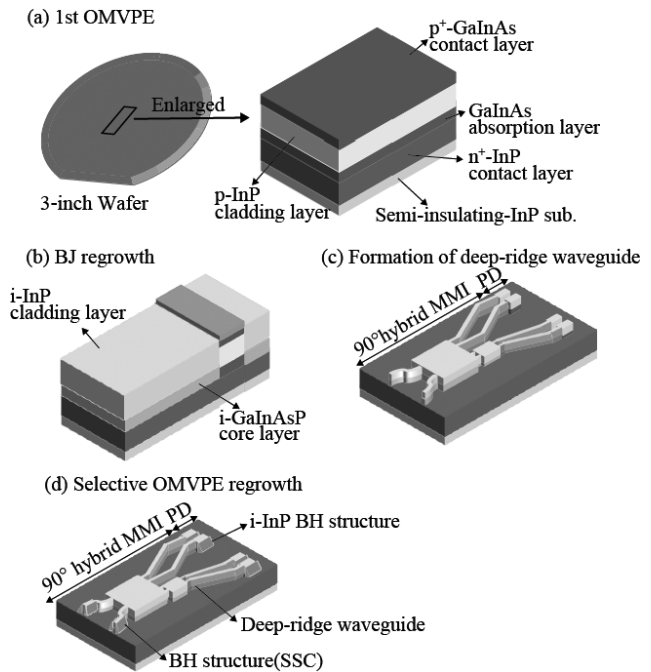


Fig. 5. Fabrication process of the InP-based photodetector monolithically integrated with the 90° hybrid

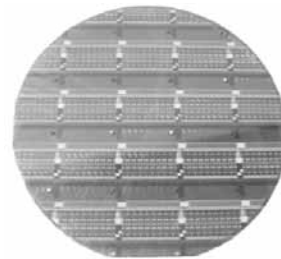


Photo. 1. Completed wafer which were fabricated the InP-based photodetectors integrated with the 90° hybrid on a semi-insulating 3-inch InP wafer (Photomicrograph)

5. Characterization

At first, discrete elements of the 90° hybrid and waveguide PDs without the 90° hybrid, that were fabricated on the same wafer with integrated devices, were evaluated. **Figure 6** shows transmittance spectra of the 90° hybrid. The variation of the loss over the C-band was less than 1.0 dB in each channel as shown in **Fig. 6**. **Figure 7** shows the phase difference, which indicates the phase deviation from 90 degrees, between the In-phase and Quadrature channels for the 90° hybrid. The phase deviation of less than ±3.0 degrees was also attained in the average of each device sample as shown in **Fig. 7**. This result indicates that the 90° hybrid consisting of 2 × 4 MMI and 2 × 2 MMI has excellent phase controllability.

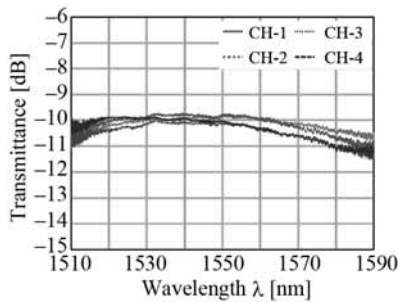


Fig. 6. Transmittance spectra of the 90° hybrid consisting of MMI

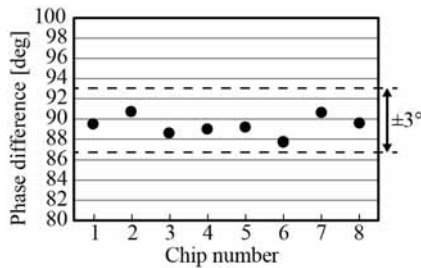


Fig. 7. Phase difference, which indicates the phase deviation from 90 degrees, between the In-phase and Quadrature channels for the 90° hybrid

Figure 8 shows the responsivity at a wavelength of 1,550 nm in each channel. Error bars indicate the standard deviation in each channel of 30 samples. The responsivity including a hybrid splitting loss of 6.0 dB, propagation loss of 0.7 dB and fiber coupling loss of 1.5 dB was as high as 0.14 A/W in the average of all samples. This high responsivity was achieved through high optical coupling efficiency with the BJ coupling structure, which consisted of the 90° hybrid and the PDs.

The accelerated aging test for the photodetector monolithically integrated with the 90° hybrid using the aforementioned process was carried out under a reverse bias voltage of 5 V at a high temperature of 175°C. The

dark current in each channel of 6 samples under a reverse bias voltage of 1.6 V at a temperature of 25°C was compared after 0, 14, 105, 335, 695, 1,050, 1,550 and 2,030 h. As a result, no noticeable changes were observed in all channels as shown in **Fig. 9**, that is, the low dark current of less than 0.2 nA was maintained after 2,000 h. The stable operation was successfully realized with InP passivation effect using the selective regrowth process. These results prove that this photodetector monolithically integrated with the 90° hybrid has sufficient properties for commercial applications of compact 100 Gbit/s coherent receivers⁽⁸⁾.

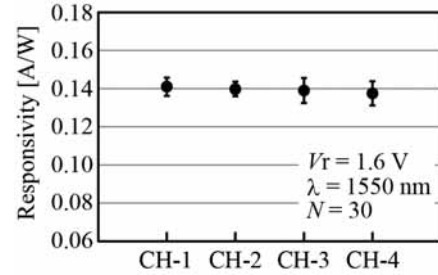


Fig. 8. Responsivity at a wavelength of 1,550 nm for a reverse bias voltage of 1.6 V in four channels of PDs monolithically integrated with the 90° hybrid

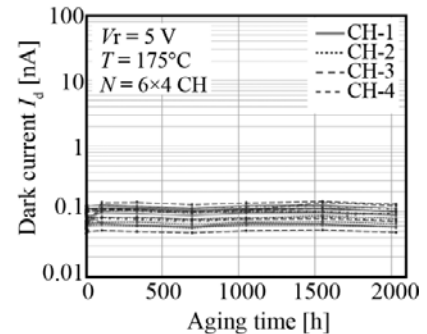


Fig. 9. Reliability test in four channels of PDs monolithically integrated with the 90° hybrid. The dark current in each aging time was measured under a reverse bias voltage of 1.6 V at a temperature of 25°C

6. Compact Coherent Receiver

Figure 10 shows (a) the schematic diagram and (b) the photograph for the fabricated polarization and phase diversity intradyne coherent receiver using the InP-based photodetectors monolithically integrated with the 90° hybrid described in Section 5⁽⁹⁾. This receiver was comprised of a beam splitter (BS), PBS, two InP-based photodetectors monolithically integrated with the 90° hybrid for transverse electric (TE) polarized light (X-polarization) and transverse magnetic (TM) polarized light (Y-polarization), and four TIAs in one package. The package body size was 15 mm × 26 mm × 5.5 mm, and it is small enough to install

the component in a 100 Gbit/s form-factor pluggable CFP/CFP2 transceiver, one of the most promising candidates for the transceiver form factor in future coherent transmission systems.

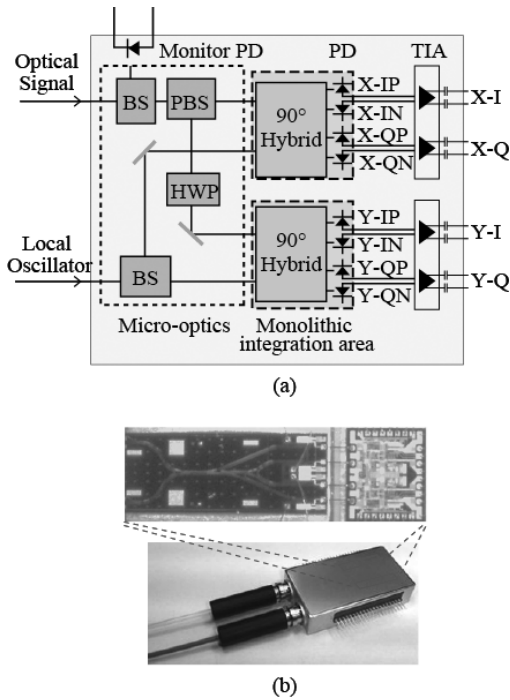


Fig. 10. (a) Schematic diagram and (b) photograph of the fabricated polarization and phase diversity intradyne coherent receiver employing the InP-based photodetectors monolithically integrated with the 90° hybrid

Figure 11 shows the responsivity, which was measured at a temperature of 25°C, of the fabricated compact coherent receiver. The receiver responsivity was as high as 0.064 A/W at a wavelength of 1,550 nm with the introduction of SSC, even though the intrinsic loss of 3 dB occurs due to separation of TE polarized light and TM polarized light in PBS. The deviation of the responsivity at 8 output channels

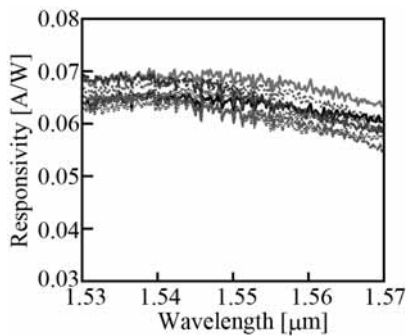


Fig. 11. Responsivity of compact coherent receiver employing the InP-based photodetector monolithically integrated with the 90° hybrid (Overwriting of 8 PD output channels)

was 0.5 dB, which indicated the uniform responsivity as shown in **Fig. 8**.

Figure 12 shows transmission characteristics using 128 Gbit/s DP-QPSK signals. **Figure 12 (a)** shows the back-to-back bit error rate (BER) vs. the optical-signal-to-noise-ratio (OSNR) for X and Y polarization. **Figure 12 (b)** shows the constellation diagram⁸ for X and Y polarization at the OSNR of 20 dB. In the OSNR measurement, 0.1 nm optical bandwidth is applied. Clear segmentation among each symbol has been measured. Hence, demodulation of 128 Gbit/s DP-QPSK modulated signals was demonstrated for the compact coherent receiver employing InP-based photodetector monolithically integrated with the 90° hybrid.

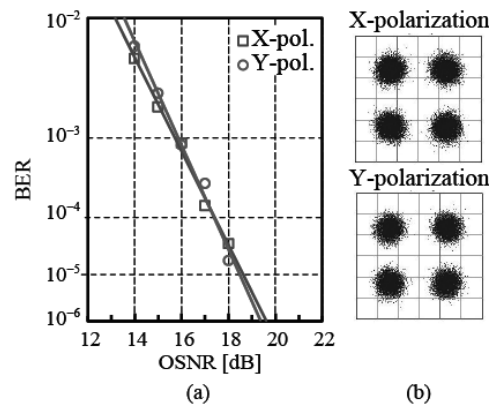


Fig. 12. (a) BER vs. OSNR curve and (b) constellation diagrams (OSNR: 20 dB) with 128 Gb/s DP-QPSK modulated signals for the coherent receiver employing the InP-based photodetector monolithically integrated with the 90° hybrid

7. Conclusion

Using InP-based monolithic integration of a 90° hybrid and waveguide photodiodes, we have developed a photodetector that provides high responsivity and high reliability. The compact coherent receiver, employing these InP-based integration devices, achieved a high sensitivity of 0.064 A/W and demodulation of 128 Gbit/s DP-QPSK modulated signals. These results reveal that the InP-based photodetector monolithically integrated with the 90° hybrid will contribute to the realization of compact coherent receivers for 100 Gbit/s and beyond transmission systems. We expect that the developed InP-based integration devices will become key devices to contribute to the revitalization of optical communication market in the future. In addition, we are convinced that our InP-based monolithic integration technologies will play an important role in the realization of higher- and more multi- functional devices.

Technical Terms

- *1 Optical Internetworking Forum (OIF): The industrial organization regarding optical communication.
- *2 CFP / CFP2: The standard of the transceiver defined by MSA about 40 / 100 Gbit/s communication.
- *3 90° hybrid: In a coherent receiver, signal light and local oscillator light interferes with each other in a 90° hybrid. A 90° hybrid outputs the interfered light for each in-phase and quadrature component.
- *4 Dual polarization-quadrature phase shift keying (DP-QPSK): QPSK is a modulation method that uses 4 phase states, which are 0, 90, 180, 270 degrees, to transmit 2 bit information in a signal time slot. DP means that a signal is multiplexed by two orthogonal polarized lights. Consequently, 4 bit information is transmitted in a signal time slot in DP-QPSK modulation method.
- *5 MMI: Multi-Mode Interferometer. The waveguide structure for multiplexing and demultiplexing of the propagation light.
- *6 Deep-ridge waveguide: The waveguide structure, which has a convex shape etched deeply on both sides, provides a strong optical confinement to a lateral direction of the waveguide.
- *7 Spot-size converter (SSC): The waveguide structure, which has a function to convert the optical mode field, is integrated to reduce the coupling loss between the device waveguide and the module optics.
- *8 Constellation diagram: A figure which express the data signal point on a two-dimensional complex plane.

References

- (1) S. Oda, T. Tanimura, T. Hoshida, C. Ohshima, H. Nakashima, Z. Tao and J. C. Rasmussen, "112 Gb/s DP-QPSK Transmission Using a Novel Nonlinear Compensator in Digital Coherent Receiver," in *Proc. OFC/NFOEC 2009*, San Diego, CA, Mar. 2009, pp. 1-3, paper OThR6.
- (2) "Implementation Agreement for Integrated Dual Polarization Intra-dyne Coherent Receivers" (IA # OIF-DPC-RX-01.2), http://www.oiforum.com/public/documents/OIF_DPC_RX-01.2 (Nov. 14, 2013)
- (3) M. Itoh and Y. Kurata, "Heterogeneous Integration of InP PDs on Silica-based PLCs," in *Proc. OFC/NFOEC 2013*, Anaheim, CA, Mar. 2013, pp. 1-3, paper OTh3H.4.
- (4) P. Dong, C. Xie, and L. Buhl, "Monolithic Coherent Receiver Based on 120-Degree Optical Hybrids on Silicon," in *Proc. OFC/NFOEC 2014*, San Francisco, CA, Mar. 2014, pp. 1-3, paper W11.5.
- (5) H. Yagi, N. Inoue, Y. Onishi, R. Masuyama, T. Katsuyama, T. Kikuchi, Y. Yoneda and H. Shoji, "High-Efficient InP-Based Balanced Photodiodes Integrated with 90° Hybrid MMI for Compact 100 Gb/s Coherent Receiver," in *Proc. OFC/NFOEC 2013*, Anaheim, CA, Mar. 2013, pp. 1-3, paper OW3L.5.
- (6) N. Inoue, H. Yagi, R. Masuyama, Y. Onishi, T. Kikuchi, T. Katsuyama, Y. Yoneda and H. Shoji, "Simultaneous Formation of Spot-Size Converters and Photodiode Waveguides to 90° Hybrid for Compact Coherent Receiver by Selective Regrowth," in *Proc. 26th IEEE Photonic Conference 2013*, Bellevue, Washington, USA, Sep. 2013, pp. 1-2, paper ThE2.4.
- (7) R. Masuyama, H. Yagi, N. Inoue, Y. Onishi, T. Katsuyama, T. Kikuchi, Y. Yoneda and H. Shoji, "Monolithic Integration of InP-Based Waveguide Photodiodes with MIM Capacitors for Compact Coherent Receiver," in *Proc. Indium Phosphide and Related Materials (IPRM) 2013*, Kobe, Japan, May 2013, pp. 1-2, paper MoD3-6.

- (8) H. Yagi, T. Kikuchi, N. Inoue, R. Masuyama, T. Katsuyama, K. Uesaka, Y. Yoneda and H. Shoji, "Highly Reliable InP-Based pin-Photodiode Array Monolithically Integrated with 90° Hybrid MMI Using Butt-Joint Regrowth," in *Proc. Indium Phosphide and Related Materials (IPRM) 2014*, Montpellier, France, May 2014, pp. 1-2, paper TuD3-2.
- (9) M. Takechi, Y. Tateiwa and S. Ogita, "Small Size 100G Coherent Receiver Using InP-based 90° Hybrid Integrated with Photodiodes," in *Proc. European Conference and Exhibition on Optical Communication (ECOC) 2013*, London, UK, Sep. 2013, pp. 1-3, paper P.2.8.

Contributors (The lead author is indicated by an asterisk (*).)

N. INOUE*

- Transmission Devices R&D Laboratories



H. YAGI

- Dr. Eng.
Assistant Manager, Transmission Devices
R&D Laboratories



R. MASUYAMA

- Assistant Manager, Transmission Devices
R&D Laboratories



T. KATSUYAMA

- Assistant General Manager, Transmission
Devices R&D Laboratories



Y. YONEDA

- Group Manager, Transmission Devices
R&D Laboratories



H. SHOJI

- Dr. Eng.
General Manager, Transmission Devices
R&D Laboratories

